The Study of Soft Soil Seismic Subsidence Based On 3D Model

Ping li (chinaliping1981@126.com)
Institute of Engineering Mechanics https://orcid.org/0000-0002-3813-8617
Junru Gu
Institute of Disaster Prevention
Yingci Liu
Institute of Disaster Prevention
Yuying Li
Institute of Disaster Prevention

Research

Keywords: ground motion, soft soil, seismic subsidence, peak ground acceleration, frequency

Posted Date: June 15th, 2021

DOI: https://doi.org/10.21203/rs.3.rs-573566/v1

Abstract

Soft soils are characterized by high sensitivity, low strength, and susceptibility to seismic subsidence. In this study, nonlinear dynamic finite element analysis was performed by OpenSees numerical simulation method to evaluate seismic subsidence response of soft soil site to input ground motions. Higher peak acceleration of ground motion enhanced degree of uneven seismic subsidence, depth of seismic depression, and damage to horizontal surface. Frequency characteristics of a ground motion are another factor influencing seismic subsidence of soft soil. Similar predominant frequency of a ground motion to natural frequency of soil site, high number of low frequency contents, and high amplitude of a ground motion promoted a more severe seismic subsidence of soft soil. The findings of this study expand current understanding on seismic subsidence of soft soil.

Introduction

Seismic subsidence of soft soil is a phenomenon in which ground or foundation subsides due to earthquake-induced softening of soft soil. Damage imposed by soft soil seismic subsidence is one of the most significant earthquake-related damages in soft soil areas. For instance, the 1976 Tangshan earthquake in China promoted seismic subsidence of buildings on soft clay foundation near Tianjin city, generated maximum settlement and inclination of 38 cm and 3% respectively (Liu Huixian 1986). In 1985, a devastating earthquake hit Mexico City and affected many buildings on soft soil. Some buildings were partially sunk by one floor, and some others had their foundations overturned (IEM 1979). These historical records indicate that earthquake-related damage in soft soil areas is primarily generated by seismic subsidence. Therefore, investigating mechanisms by which ground motion promotes soft soil subsidence is important for mitigating earthquake damage in soft soil areas.

Factors influencing seismic subsidence of soft soil have been extensively investigated. Seed H.B. and. Chan C.K. (1966) found that soil samples consolidated under a static pressure produced additional deformation under dynamic stress. Yu Shousong and Shi Zhaoji (19189)suggested that soil seismic subsidence was related to amplitude of dynamic stress, vibration time, consolidation stress, and soil type. Chen Guoxing (2004) reported that base pressure, ground motion intensity, foundation size, buried depth of foundation, and foundation form determined seismic settlement of a foundation. Meng Shangjiu and Yuan Xiaoming (2004)proposed that uneven seismic subsidence of buildings was resulted from combined effect of soft soil layers, uneven load distribution of buildings, and ground motion waveforms. Among these factors, the authors pointed out that asymmetry and irregularity of ground motion waveforms were the most important contributing factors to uneven seismic subsidence. By centrifuge analyses on soft solid foundation, Zhou Yan-guo and Zhou Yanguo and Chen Yunmin (2009) indicated that structural asymmetry and overburden loads of buildings promoted uneven seismic subsidence. Li Nan (2002) reported that soft soil subsidence was affected by amplitude of ground motion, site conditions, and overburden loads. Based on available soil engineering and numerical simulation studies, several factors encompassing upper load, soil layer characteristics, ground motion characteristics, and site characteristics were proposed to be influencing factors of soft soil seismic subsidence. However, in

view of complex properties of saturated soft clay (high sensitivity, strong compressibility, low water permeability, and low strength), there are yet extensive evidences on the effect of aforementioned factors, particularly impact of ground motion characteristics, on soft soil seismic subsidence. Therefore, this study adopted OpenSees finite element analysis software to create a three-dimensional model of soft soil site and apply numerical simulation for studying effect of peak acceleration and frequency characteristics of ground motion on soft soil subsidence. The findings of this study enhance existing understanding on mechanism of soft soil subsidence and serve as a guidance for seismic design of soft soil foundation.

Materials And Method

Design of three-dimensional model of soft soil site

A three-dimensional model of soft soil site and schematic diagram of the monitoring points are presented in Fig. 1. Dimensions of the site are 30 m (length) × 30 m (width) × 12 m (height) to reduce calculation time and ensure stability of calculated values (Liao Zhenpeng 2004) Size of horizontal and vertical grid is determined to be 1 m and 0.5 m respectively. A three-story frame structure exerting a load of 80 kPa on upper section of the site constitutes the full, simplified three-dimensional model of soft soil site. A rigid boundary is selected for the bottom of the model, and an undrained boundary is set on the surface. Upper and bottom section of the model and foundation-foundation contact surface adopt forced displacement boundaries to keep soil around the model and soil in contact with foundation-foundation boundary maintain synchronous displacement.

The three-dimensional model adopts the above-mentioned PIMY soil constitutive model, and the soil is twenty-node hexahedral (Twenty_Eight_Node_BrickUP) based on Biot's porous media theory. This study focuses on impact of ground motion characteristics on soft soil subsidence. Therefore, empirical parameters of soft soil are calculated and presented in Table 1 (Yang Z. et al. 2004). Initially, elasticity during initial ground stress field was calculated by applying gravity. Subsequently, UpdateMaterial command was applied to calculate permanent deformation. Eventually, ground motion load was imposed for dynamic analysis.

Table 1
Empirical parameter values of soft soil site model

Parameter	Value
Density (ton/m^3)	1.3
Shear modulus (kPa)	1.3×10^4
Bulk modulus (kPa)	6.5×10^4
Cohesion (kPa)	18
Peak shear strain	0.1
Fraction angle (°)	0
Confining pressure (kPa)	100
Yield surface numbers	20

Input ground motion

Consistent excitation method was selected to apply El Centro ground motion (Imperial Valley earthquake, 1940) from horizontal direction to the bottom of the model and obtain seismic subsidence response. Time history curve and Fourier spectrum of the ground motion are shown in Fig. 2. Peak ground acceleration (0.319 g) appears at 2.02 s. On the other hand, low frequency below 10 Hz predominates Fourier spectrum of the ground motion. Amplitude of the Fourier spectrum is situated between 1–2 Hz. In order to study impact of PGA on soft soil subsidence, PGA of EL Centro ground motion was adjusted to 0.15 g, 0.30 g, and 0.40 g.

In addition to the El Centro ground motion, two similarly popular ground motions (Kobe and Taft ground motion) were incorporated to study influence of frequency characteristics of ground motion on soft soil subsidence. PGA of the Kobe and Taft ground motion was adjusted to 0.3 g for performing numerical simulations. Time history curve and Fourier spectrum of Kobe ground motion (Hyogoken-Nanbu earthquake, 1995) are shown in Fig. 3. On the other hand, time history curve and Fourier spectrum of Taft ground motion (California earthquake, 1952) are presented in Fig. 4. Fourier spectra of Kobe and Taft ground motion are predominated by low-frequency below 5 Hz. and below 8 Hz respectively.

Methods of analysis

OpenSees is an object-oriented, open-source finite element analysis software which is widely used in earthquake engineering. Source code of OpenSees is completely open, and users are able to select or re-develop available constitutive model, unit form, and solution algorithm.

In this study, PIMY model was selected as soil constitutive model. PIMY model illustrates plasticity of elastoplastic materials under deviatoric stress-strain conditions. The model exhibits linear-elastic volumetric stress-strain response and is not affected by deviatoric response. PIMY model simulates response of materials, which shear behavior is not sensitive to confinement changes, to monotonic or cyclic loading (Yang Z. et al.2003).

Figure 5 shows stress-strain behavior of PIMY model. During application of gravity load (i.e., consolidation stage), the model exhibits linear elasticity. During subsequent dynamic loading stage, the model demonstrates elastoplastic stress-strain response. Plasticity of the model is calculated based on multiple yield surface principle and the corresponding flow law. The yield surface obeys VonMises yield criterion.

Results And Discussion

Influence of PGA of ground motion on seismic subsidence of soft soil

Vertical displacement of soil due to input El Centro ground motion with PGA of 0.15g was calculated at the bottom of the foundation for each monitoring point. Figure 6 shows seismic subsidence of ground surface derived from dynamic calculation on three-dimensional model of the soft soil site Fig. 6a suggests that the seismic subsidence propagates from the center, at which the most significant seismic displacement was observed, and gradually decreases until reaching ground surface at which significant plastic deformation and shear failure were observed. Figure 6b illustrates cross-sectional view of the foundation after seismic subsidence. Propagation of the seismic subsidence assumes a parabolic shape symmetrically distributed on the sides with low middle and high sides, and maximum depression angle of 3.44°. The largest vertical displacement is observed at bottom center section of the foundation. Impact distance of the seismic subsidence is elliptical, spanning from 5–25 m in X-direction and 6–24 m in Y-direction. Soil on X-direction and Y-direction of the foundation is compressed and uplifted by 15mm.

Vertical displacement of soil due to input El Centro ground motion with PGA of 0.30 g was calculated at the bottom of the foundation for each monitoring point. Figure 7 shows seismic subsidence of ground surface derived from dynamic calculation on three-dimensional model of the soft soil site. Figure 7a indicates that the seismic subsidence spreads from the center, at which the largest subsidence was observed, and gradually decreases until reaching ground surface at which significant plastic deformation and shear failure were recorded. Figure 7b illustrates cross-sectional view of the foundation after seismic subsidence. Propagation of the seismic subsidence adopts a parabolic shape symmetrically distributed on the sides with low middle and high sides, and maximum depression angle of 7.91°. Bottom middle section of the foundation demonstrates the largest vertical displacement. Impact range of the seismic subsidence is elliptical, covering 4.5–25.5 m in X-direction and 6.5–24.5 m in Y-direction. Soil on X-direction and Y-direction of the foundation is compressed and uplifted by 35mm.

Vertical displacement of soil due to El Centro ground motion with a PGA of 0.40g was calculated at the bottom of the foundation for each monitoring point. Figure 8 shows seismic subsidence of ground surface derived from dynamic calculation on three-dimensional model of soft soil site. Figure 8a implies that seismic subsidence propagates from the center, at which the most significant seismic subsidence was recorded, and gradually decreases until reaching ground surface at which significant plastic deformation and shear failure were detected. Figure 8b illustrates cross-sectional view of the foundation after seismic subsidence. Propagation of the seismic subsidence assumes a parabolic shape symmetrically distributed on the sides with low middle and high sides, and maximum depression angle of 8.0°. Bottom center section of the foundation exhibits the largest vertical displacement. Impact area of the seismic subsidence is elliptical, ranging from 4.5–26.0 m in X-direction and 6.0–25.0 m in Y-direction. Soil on X-direction and Y-direction of the foundation is compressed and uplifted by 46 mm.

Overall effects of PGA of ground motion on soft soil seismic subsidence are summarized in Fig. 9–11. As shown in Fig. 9, seismic subsidence generated by 0.15 g ground motion is approximately 104mm, which is 80.6% and 148.6% lower than the subsidence generated under the action of 0.3 g and 0.4 g ground motion (189 mm and 260 mm). This indicates that increase in PGA distinctly increases degree of seismic subsidence. Figure 10 illustrates development of seismic subsidence at different depth of soil. Lower seismic subsidence is observed at deeper soil layer. Nevertheless, 0.4 g ground motion produces notably higher seismic subsidence than 0.15 and 0.3 g ground motion regardless of the soil depth, indicating a non-linear stress-strain response of the soil.

PGA of ground motion influences uneven surface subsidence. As suggested in Fig. 11, the larger is the PGA, the more significant is the subsidence, the higher is the uplifted distance of soil on X-direction and Y-direction of the foundation, and the larger is the damage distance on horizontal surface. Impact of the seismic subsidence is larger in X-direction than Y-direction, as a consequence of the direction to which input ground motion is applied.

Influence of frequency characteristics of ground motion on soft soil seismic subsidence

Figure 12 shows seismic subsidence of ground surface derived from dynamic calculation on three-dimensional model of soft soil site. The seismic subsidence propagates from the center, at which the largest subsidence was observed, and gradually decreases until reaches ground surface at which significant plastic deformation and shear failure were indicated. Figure 12b illustrates X-direction and Y-direction cross-section of the foundation after the seismic subsidence. Propagation of the subsidence adopts overall parabolic shape symmetrically distributed on the sides with low middle and high sides, and maximum depression angle of 5.01°. The largest displacement was documented at bottom middle section of the foundation. Impact distance of the subsidence is elliptical, spanning from 4.5-25.5 m in X-direction and 6.0-25.0 m in Y-direction. Soil on X-direction and Y-direction of the foundation is compressed and uplifted by 24 mm.

Vertical displacement of soil due to input Taft ground motion with PGA of 0.30 g was calculated at the bottom of the foundation for each monitoring point. Figure 13 shows seismic subsidence of ground surface derived from dynamic calculation on three-dimensional model of soft soil site. Figure 13a suggest that the seismic subsidence spreads from the center, at which the largest subsidence was observed, and gradually decreases until reaches ground surface at which plastic deformation and shear failure were recorded. Figure 13b illustrates cross-sectional view of the foundation after seismic subsidence. The subsidence adopts an overall parabolic shape symmetrically distributed on the sides with low middle and high sides, and maximum depression angle of 7.66°. The largest vertical displacement was observed at bottom middle section of the foundation. Impact distance of the seismic subsidence is elliptical, ranging from 4.5–26.0 m in X-direction and 6.5–25.0 m in Y-direction. Soil on X-direction and Y-direction of the foundation is compressed and uplifted by 44mm.

Overall effects of frequency characteristics of ground motion on soft soil seismic subsidence are summarized in Fig. 14–16. Figure 14 shows that the three ground motions (EL Centro, Kobe, and Taft) produced vertical displacement curves with different growth characteristics. Kobe ground motion initiates soil subsidence at 7 s, which is consistent with onset time at which PGA of the Kobe ground motion is recorded. Figure 15 shows development of seismic subsidence at different depth of soil. Regardless of the soil depth, Taft ground motion demonstrates the most significant seismic subsidence followed by El Centro and Kobe ground motion.

Figure 16 indicates that the three ground motions generated different degrees of seismic subsidence, which suggests the influence of frequency characteristics of the ground motions on soft soil seismic subsidence. Natural frequency of the model site is 1.2 Hz. Similarly, amplitude of Fourier spectrum of Taft ground motion is located at 1–2 Hz, which is close to natural frequency of the site. This resonance significantly increases vertical displacement of soil. Despite exhibiting many low-frequency contents similar to the Taft ground motion, El Centro and Kobe ground motion demonstrate lower amplitude than the Taft ground motion. Therefore, Taft ground motion produced the most severe soft soil seismic subsidence among the investigated ground motions. Overall, these findings highlight the significance of low-frequency contents and amplitude of Fourier spectrum on soft soil seismic subsidence. Higher abundance of low-frequency contents and higher amplitude of Fourier spectrum promote a more severe seismic subsidence.

Despite this study contributes towards understanding on impact of PGA and frequency characteristics of ground motion on soft soil subsidence, these findings were derived from a simplified three-dimensional model. Hence, there may be mechanisms and/or factors related to actual soft soil subsidence during strong earthquakes, which are unaccounted by current model. On this account, a large-scale three-dimensional model which simulates actual interaction between foundation and soft soil is necessary to obtain more reliable conclusions from numerical analysis. Moreover, further research is encouraged to account for soft soil properties, upper load, and foundation-soil interaction for validating impact of ground motion characteristics on soft soil and deriving influencing factors of soft soil seismic subsidence.

Conclusion

A three-dimensional model of soft soil site was established, and finite element numerical calculation was carried out to evaluate influence of PGA and frequency characteristics of ground motion on seismic subsidence of soft soil. Higher PGA of ground motion increases degree of seismic subsidence, depth of seismic depression, and damage to horizontal surface. Frequency characteristics of ground motion are a similarly important influencing factor of soft soil subsidence. Higher number of low frequency contents and higher amplitude of ground motion generate a more severe seismic subsidence. Moreover, the more similar is the predominant frequency of a ground motion to natural frequency of soft soil site, the more significant is the seismic subsidence.

Declarations

Availability of data and materials

IEM: Institute of Engineering Mechanics Chinese Academy of Science; OpenSees :Open System for Earthquake Engineering Simulation; PGA: peak ground acceleration; PIMY :Pressure Independ Multi Yield model.

Competing interests

The authors declare that they have no competing interests.

Funding

China earthquake administration Spark Project of Earthquake Science and Technology (XH204401) has funded for analysis and construction.

Authors' contributions

Ping Li was involved in simulations and writing the manuscript. And all other author contributed in data analysis, simulations and writing the paper. The author(s) read and approved the final manuscript.

Acknowledgements

The authors would like to thank China earthquake administration Spark Project of Earthquake Science and Technology for funding Authors would like to acknowledge Opensees for providing numerical method.

Author details

[1] Key Laboratory of Earthquake Engineering and Engineering Vibration, Institute of Engineering Mechanics, China Earthquake Administration , Haerbin150081, Heilongjiang Province, China

[2]Institute of Disaster Prevention, Sanhe, Hebei province 065201, China

[3] Sichuan Metallurgical Geological Survey and Design Group Co., Ltd, Chengdu, 610081, China

4 Hebei Key Laboratory of Earthquake Disaster Prevention and Risk Assessment, Sanhe 065201

References

1. Chen G (2004) A simplified method for calculating earthquake-induced foundation subsidence of multi-storied buildings and analysis of influencing factors. Journal of Disaster Prevention Mitigation Engineering 24(1):47–52 (in Chinese)
2. Liu H (1986) Tangshan Earthquake damage. Seismological Press, Beijing (in Chinese)
3. Institute of Engineering Mechanics Chinese Academy of Science(IEM) (1979) Haicheng Earthquake damage. Seismological Press, Beijing (in Chinese)
4. Li Nan((2002) Based on the subsidence of soft soil and its influencing factors of OpenSees research]. Institute of Engineering Mechanics, China Earthquake Administration, Haerbin, (in Chinese)
5. Liao Zhenpeng (1997) Numerical simulation of near-field wave. Advances in Mechanics 27(2):193–212 (in Chinese)
6. Meng Shangjiu and Yuan Xiaoming(2004)The research to the influential factors of differential subsidence of buildings. Earthquake Engineering and Engineering Vibration, 24(1): 111–116 (in Chinese)Seed H.B and Chan CK (1966) Clay strength under earthquake loading condition. Journal of the Soil Mechanics and Foundations Division, ASCE, (92): (SM2)
7. Yang Z, Lu J, Elgamal A (2004)A web-based platform for live internet computation of seismic ground response, Advances in Engineering Software, 2004, 35, 249–259
8. Yang Z, Elgamal A, Parra E (2003) Computational model for cyclic mobility and associated shear deformation. Journal of Geotechnical Geoenvironmental Engineering American Society of Civil Engineering 129(12):1119–1127
9. Yu Shousong and Shi Zhaoji (1989) The soil subsidence of experimental research. Chinese Journal of Geotechnical Engineering, 11(4):35–44 (in Chinese) Zhou Yanguo and Chen Yunmin(2009)Building on soft clay foundation uneven settlement centrifuge test research. Chinese Science, 39(6):1129–1137 (in Chinese)

Figures

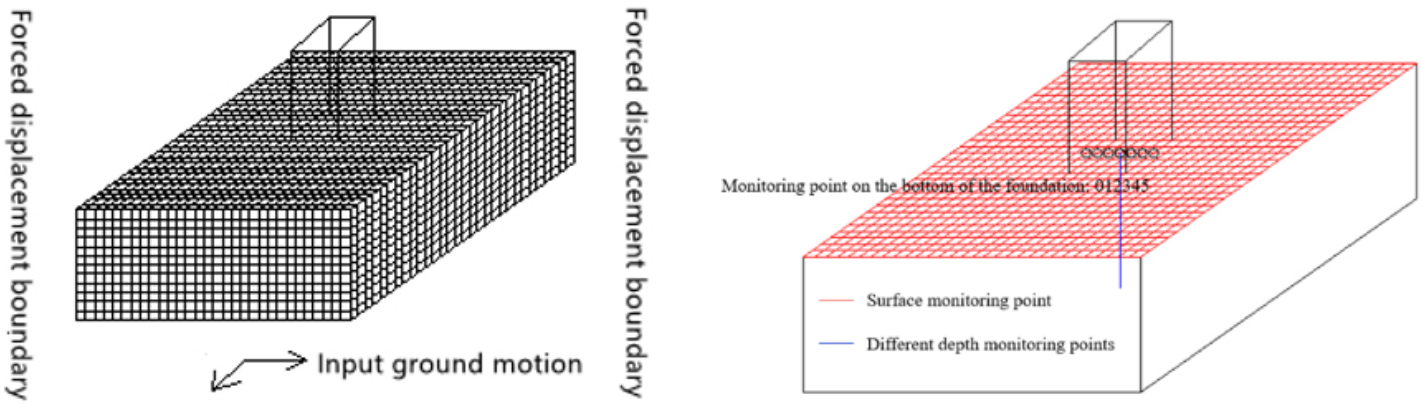

Figure 1

Schematic diagram on three-dimensional model of soft soil site

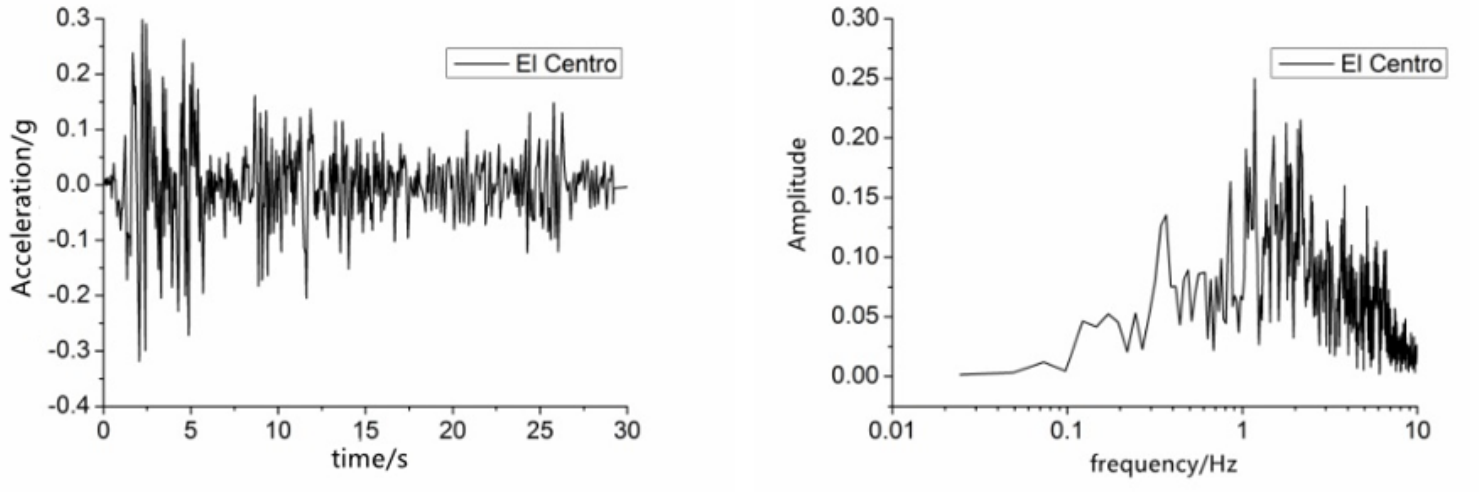

Figure 2

Time history curve and Fourier spectrum of El Centro ground motion

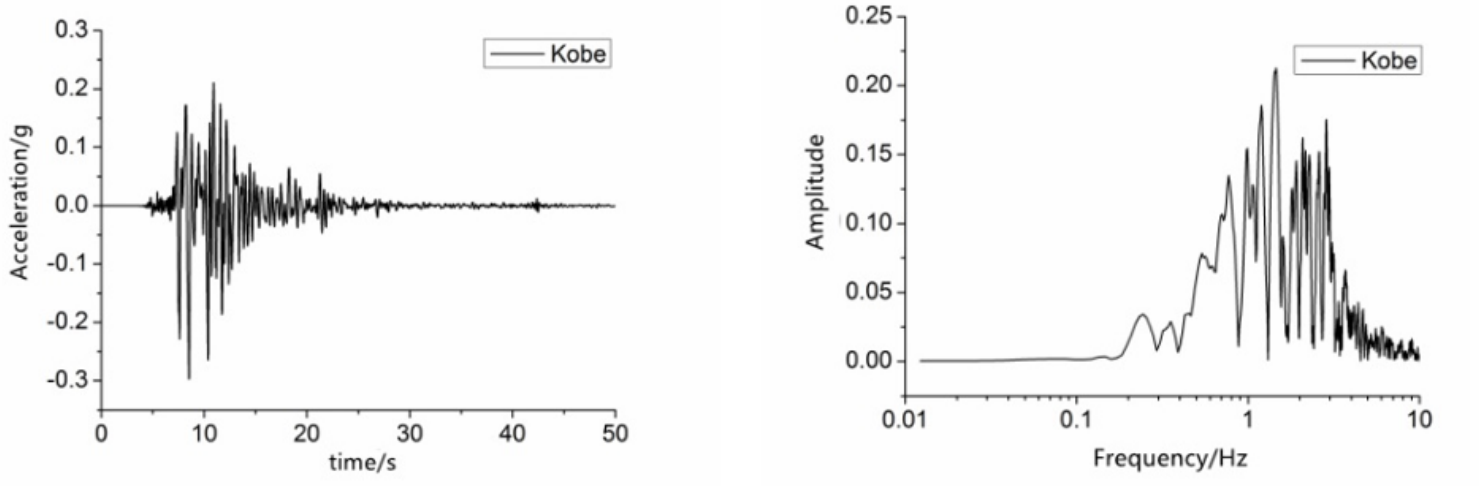

Figure 3

Time history curve and Fourier spectrum of Kobe ground motion

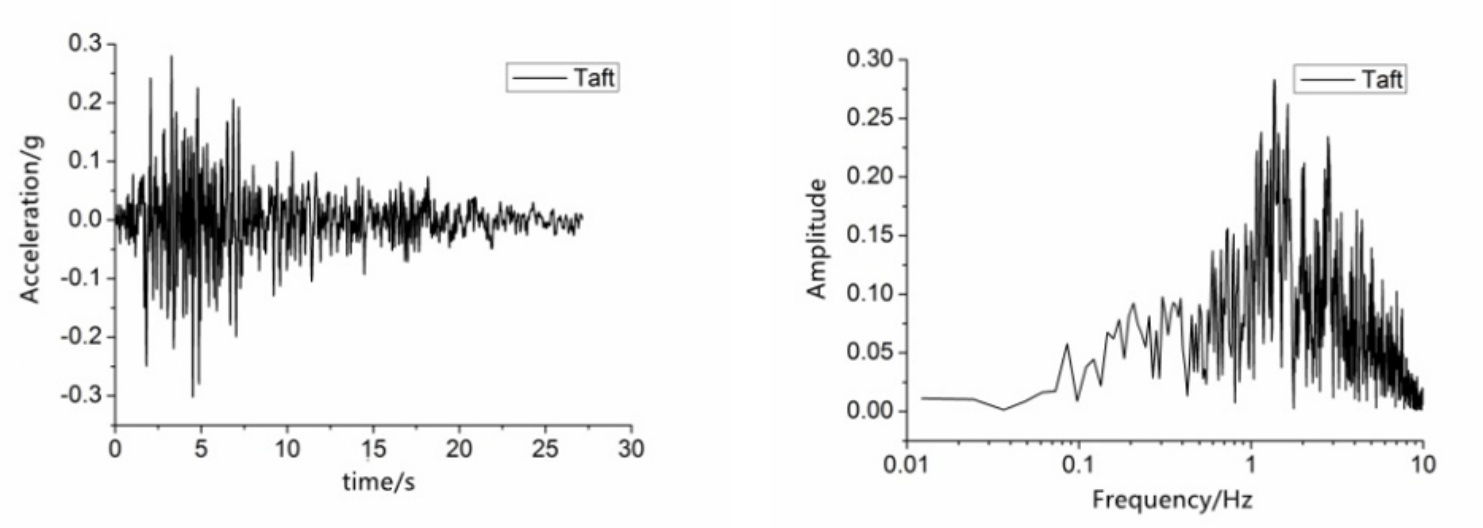

Figure 4

Time history curve and Fourier spectrum of Taft ground motion

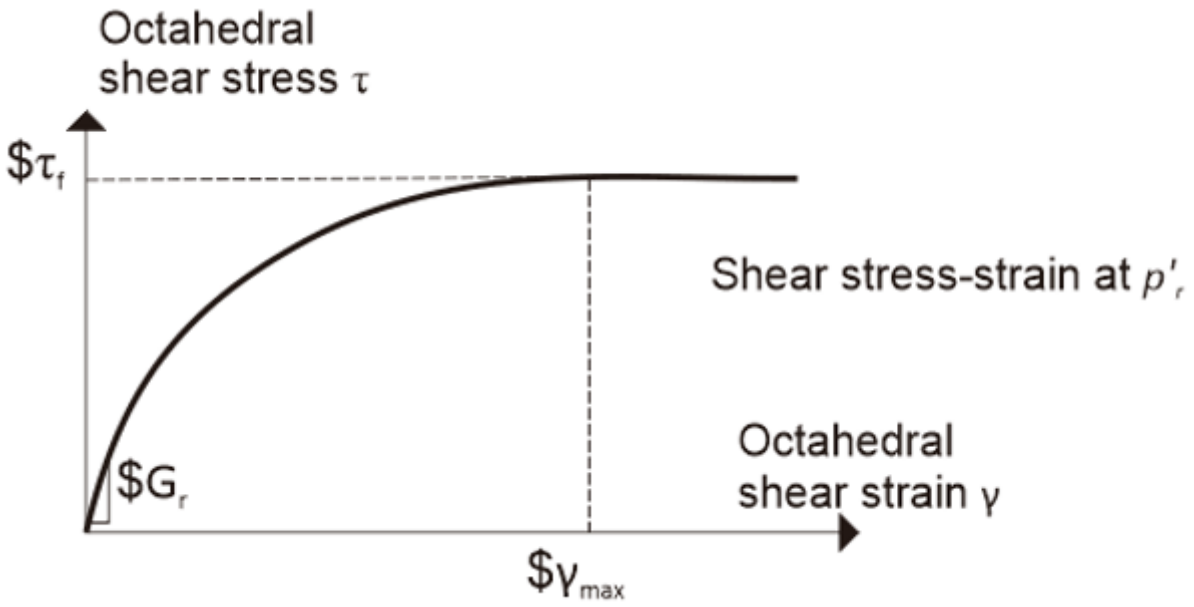

Figure 5

Stress-strain behavior of PIMY model

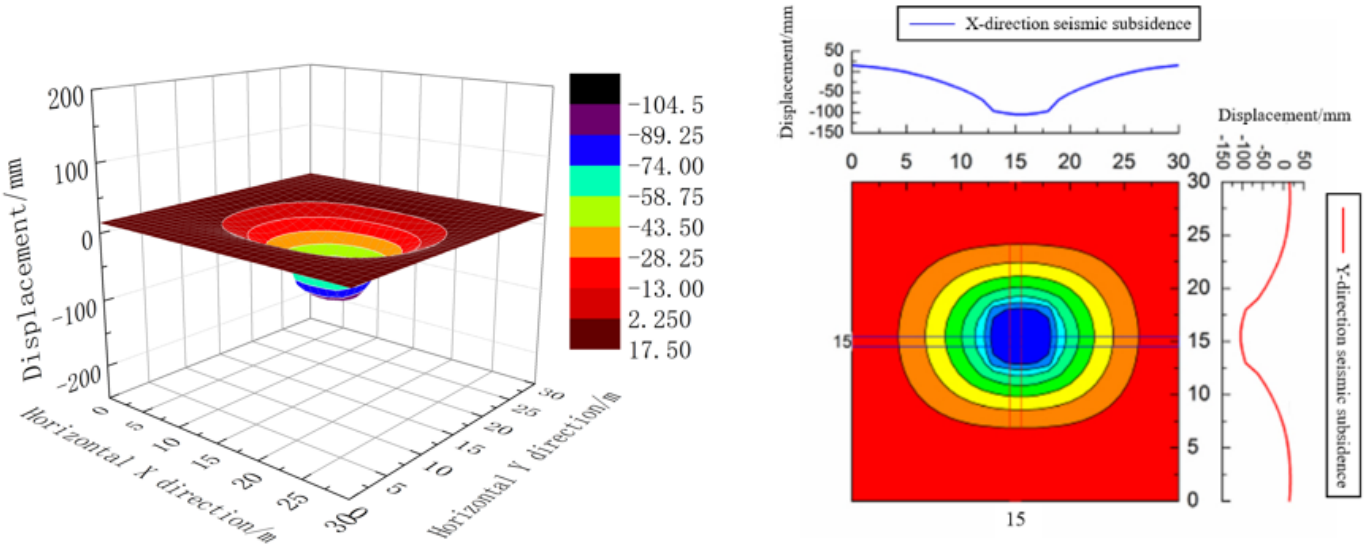

(a) Full view (b) Cross-sectional view

Figure 6

Seismic subsidence of ground surface due to input 0.15 g El Centro ground motion

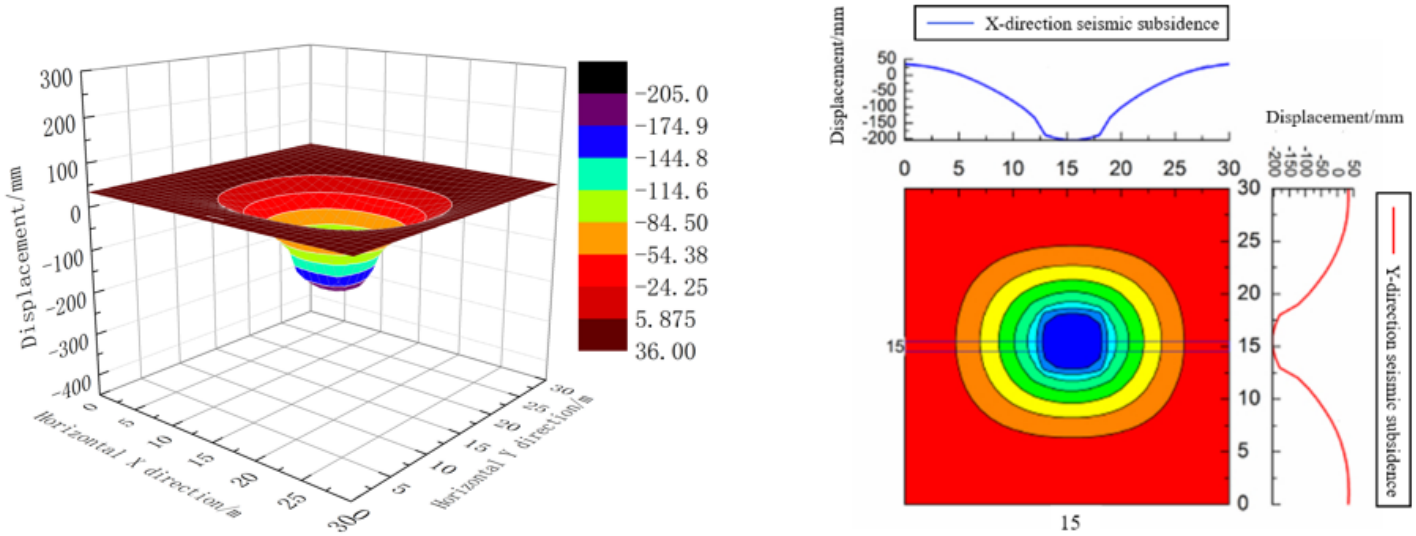

(a) Full view (b) Cross-sectional view

Figure 7

Seismic subsidence of ground surface due to input 0.30 g El Centro ground motion

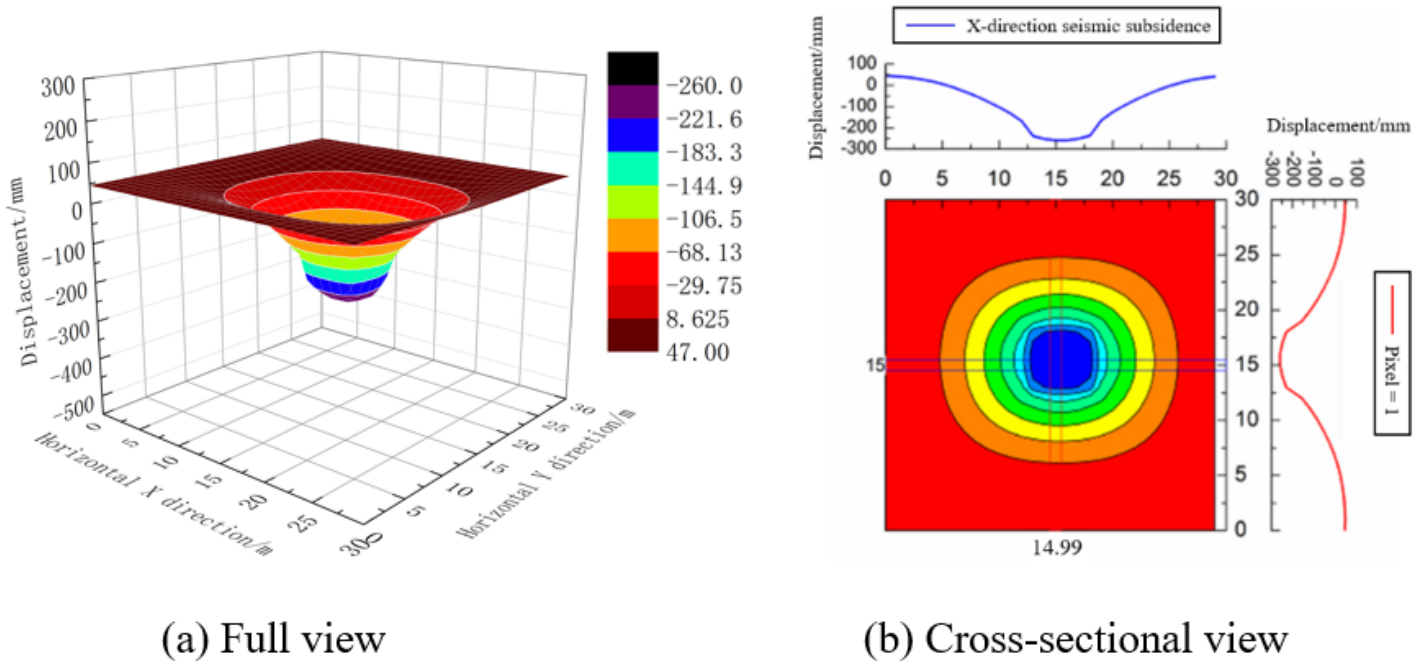

Figure 8

Seismic subsidence of ground surface due to input 0.40g El Centro ground motion

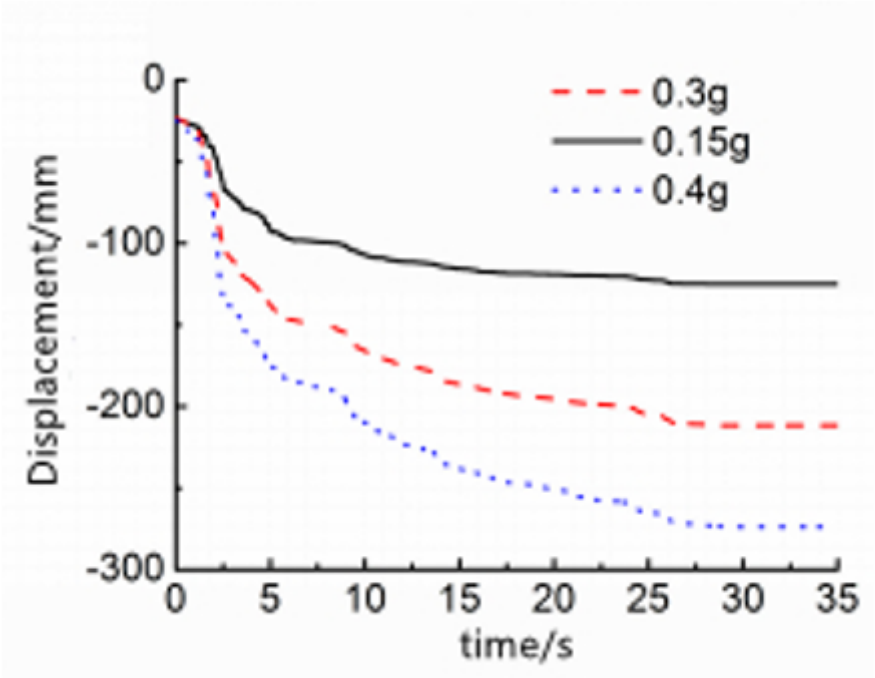

Figure 9

Time history curve illustrating vertical subsidence of soil due to input El Centro ground motion with various PGA

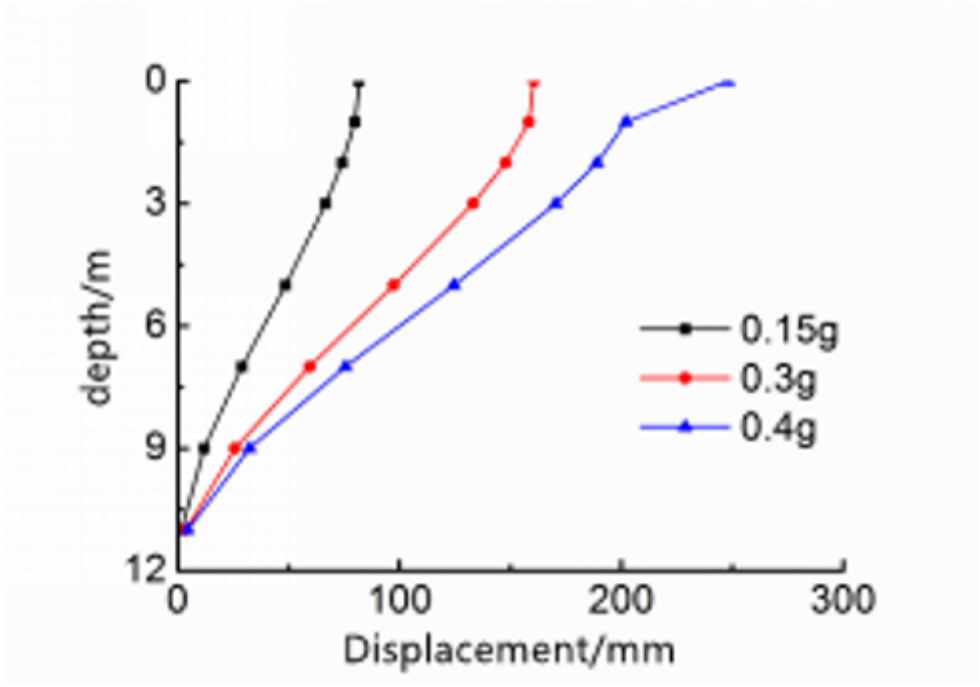

Figure 10

Seismic subsidence at different soil depth due to El Centro ground motion with different PGA

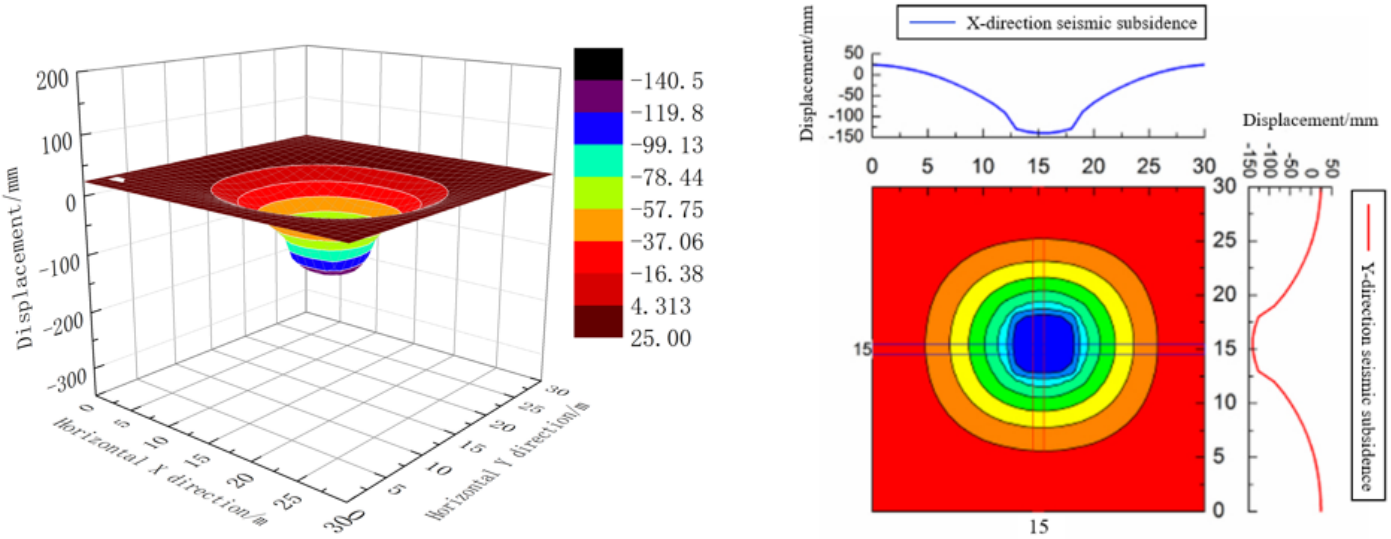

(a) Full view (b) Cross-sectional view

Figure 12

Seismic subsidence of ground surface due to input 0.30 g Kobe ground motion

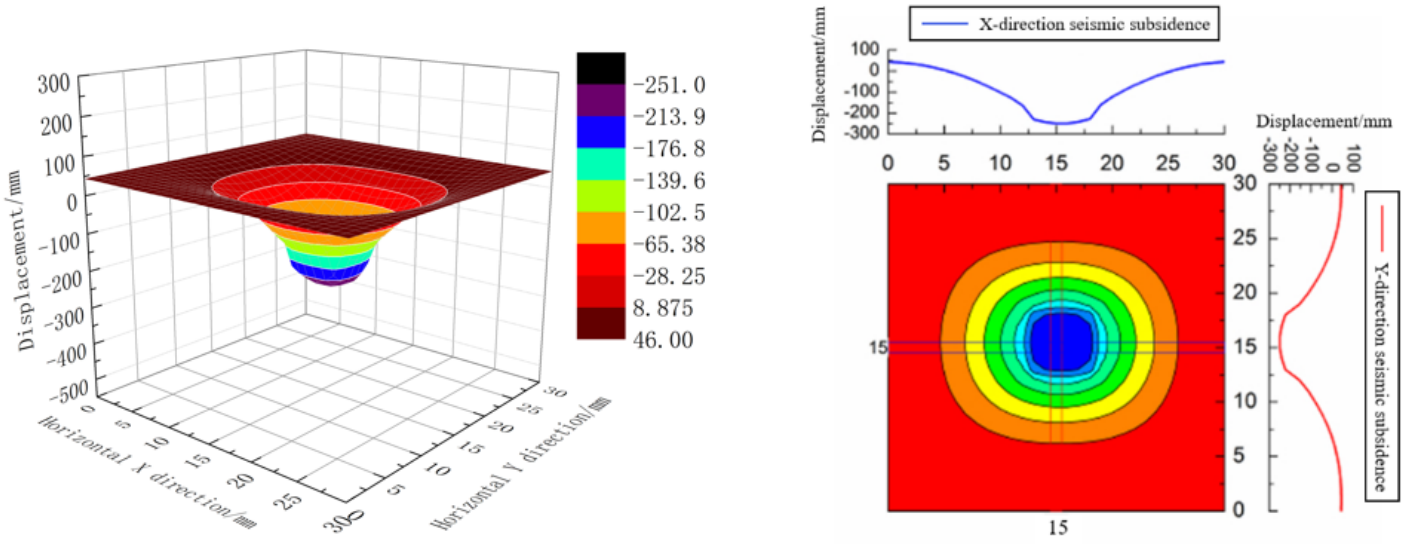

(a) Full view (b) Cross-sectional view

Figure 13

Seismic subsidence of ground surface due to input 0.30 g Taft ground motion

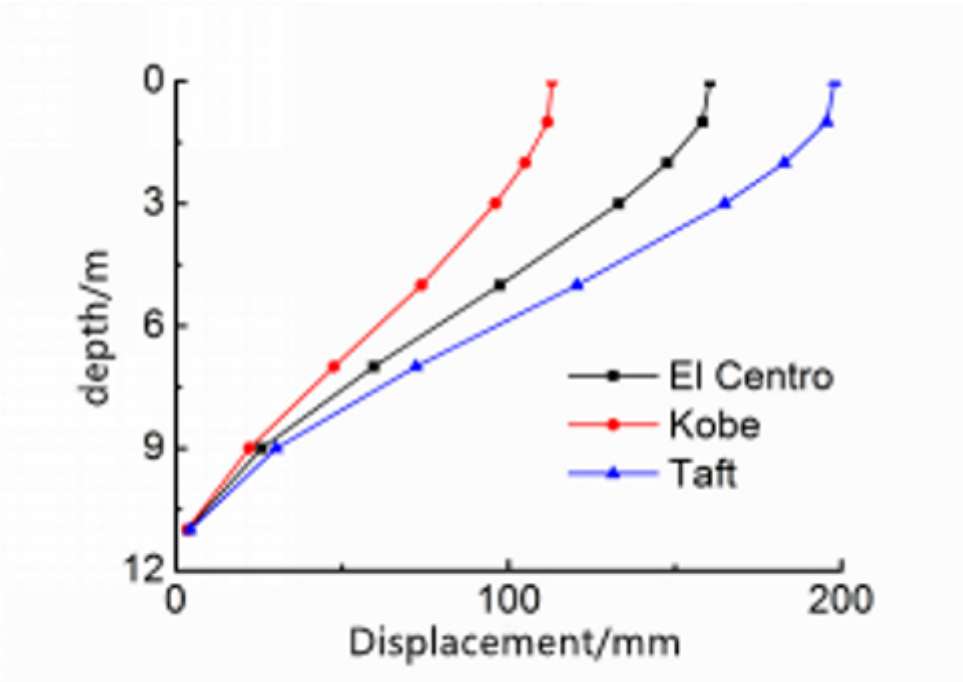

Figure 15

Seismic subsidence at different soil depth due to different ground motions

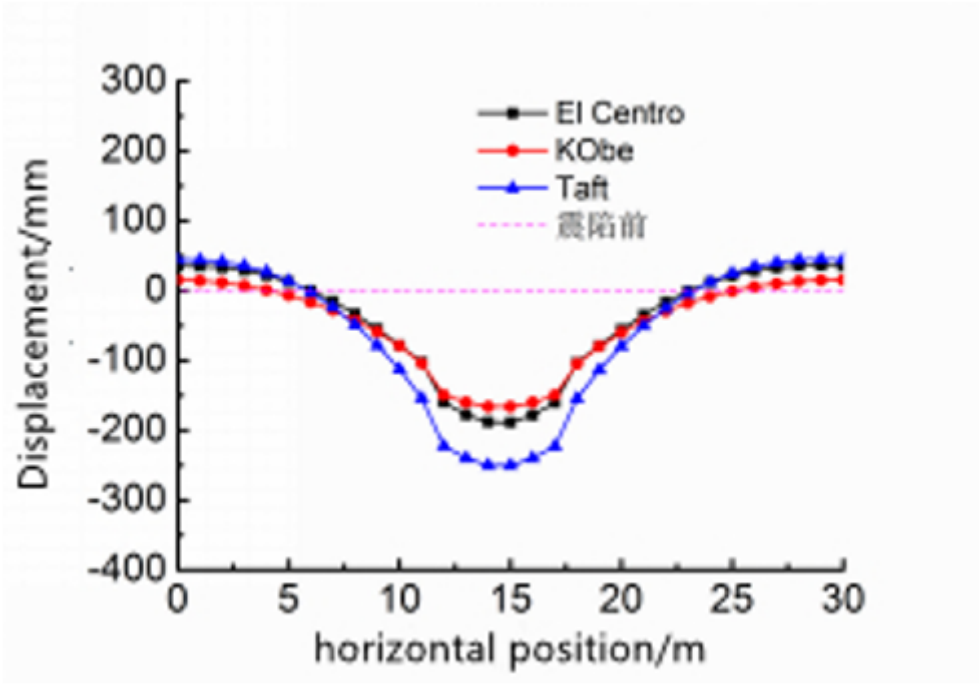

Figure 16

Uneven seismic subsidence due to different ground motions